Journal of Nuclear Materials 389 (2009) 402–406

Contents lists available at ScienceDirect

Journal of Nuclear Materials

journal homepage: www.elsevier.com/locate/jnucmat

Effect of oxygen potential on the sintering behavior of MgO-based heterogeneous fuels containing $(Pu,Am)O_{2-x}$

Shuhei Miwa *, Yohei Ishi, Masahiko Osaka

Oarai Research and Development Center, Japan Atomic Energy Agency, 4002 Narita-cho, Oarai-machi, Higashi-Ibaraki-gun, Ibaraki 311-1393, Japan

ARTICLE INFO

Article history:
Received 2 September 2008
Accepted 9 February 2009

ABSTRACT

The effect of oxygen potential on the sintering behavior of MgO-based heterogeneous fuels containing $(Pu,Am)O_{2-x}$ was experimentally investigated. Sintering tests in various atmospheres, i.e. air, moisturized 4%H_2–Ar, and 4%H_2–Ar atmosphere, were carried out. The sintering behavior was found to be significantly affected by the oxygen potential in the sintering atmosphere. The sintered density decreased with decreasing oxygen potential. The $(Pu,Am)O_{2-x}$ phase sintered in a reductive atmosphere had hypostoichiometry. The aggregates of the $(Pu,Am)O_{2-x}$ phase sintered in the reductive atmosphere grew, in comparison with those in the oxidizing one. The sintering mechanism was discussed in terms of the difference in sintering behavior of $(Pu,Am)O_{2-x}$ and MgO.

© 2009 Elsevier B.V. All rights reserved.

1. Introduction

Heterogeneous fuels with a high content of minor actinides (MAs) are currently considered as one promising option for the rapid incineration of MAs in a future fast reactor cycle system [1,2]. Heterogeneous fuels are a composite of MA oxide host phase and an inert matrix (IM). Magnesium oxide (MgO) is considered to be a promising candidate for an IM since it has a high melting temperature and relatively high thermal conductivity, which can lead to a low operating temperature and large safety margin in the case of accidental melting of fuel [1–3]. In addition, MgO has high adaptability to a powder metallurgy which can simplify the fabrication procedure. This is preferable characteristics especially as an IM for the rapid deployment of the heterogeneous fuels, since the powder metallurgy could be adapted to the presently used commercial manufacturing technology [4,5]. In addition, such a simple fabrication procedure is indispensable for MA-containing fuels since they must be fabricated inside a shielded and air-tight cell by remote handling.

In order to take advantage of the high performance of MgO matrix, a high density of the heterogeneous fuels is a prerequisite. However, unlike homogeneous fuels such as UO_2 and mixed oxide (MOX), the host phase can retard the densification of IM [6–8]. Therefore, in order to obtain the high density fuel, the matching of densification behavior between the host phase and the IM phase is required [9]. On the other hand, the densification behavior of nuclear oxide fuels, such as UO_2, PuO_2 and MOX which have a fluorite structure, is known to be affected by oxygen potential in the sintering atmosphere [10–12]. Therefore, the sintering behavior of the heterogeneous fuels containing such a fluorite-type oxide should be affected by oxygen potential in the sintering atmosphere. Furthermore, some characteristics of Am-containing oxide compounds, such as $(U,Pu,Am)O_{2-x}$ and $(Pu,Am)O_{2-x}$ have been reported to show unique behavior [13–16], which is attributable to the higher oxygen potential of Am-containing oxide compounds compared with UO_2, PuO_2 and MOX fuels [13,15,17]. As an example, the sintering behavior of $(U,Pu,Am)O_{2-x}$ was found to be significantly affected by oxygen potential which was attributed to the high oxygen potential of $(U,Pu,Am)O_{2-x}$ [14]. These results indicated that the sintering behavior of MgO-based heterogeneous fuels containing Am-containing oxides should be significantly affected by oxygen potential in the sintering atmosphere. Therefore, it is important to investigate the effect of the oxygen potential in the sintering atmosphere on the sintering behavior of MgO-based heterogeneous fuels containing Am-containing oxides. In this study, the sintering behavior of MgO-based heterogeneous fuels containing $(Pu,Am)O_{2-x}$ ($(Pu,Am)O_{2-x}$–MgO) was experimentally investigated. Sintering tests in various atmospheres were carried out, and the sintering mechanism was discussed in terms of the difference in sintering behavior between $(Pu,Am)O_{2-x}$ and MgO.

2. Experimental

Table 1 shows the characteristics of $(Pu,Am)O_2$ and MgO powders. 9 wt% of ^{241}Am was generated in $(Pu,Am)O_2$ powder by beta-decay of ^{241}Pu. MgO powder (about 0.1 μm particle diameter) was supplied by Ube Material Industry Co. Ltd. Fig. 1 shows the fabrication procedure for $(Pu,Am)O_{2-x}$–MgO pellets. The fabrication procedure is based on conventional powder metallurgy. It consists of the following steps: heat treatment of $(Pu,Am)O_2$ powder at 903 K, milling of the $(Pu,Am)O_2$ powder in a ball mill for 3 h

* Corresponding author. Tel.: +81 29 267 4141; fax: +81 29 266 0016.
E-mail address: miwa.shuhei@jaea.go.jp (S. Miwa).

0022-3115/$ - see front matter © 2009 Elsevier B.V. All rights reserved.
doi:10.1016/j.jnucmat.2009.02.016

Table 1
Characteristics of $(Pu,Am)O_2$ and MgO powders.

	$(Pu,Am)O_2$	MgO[a]
Composition	$(Pu_{0.91}Am_{0.09})O_2$	MgO
Total impurities (ppm)	<883	<113
Particle radius (μm)	2.83	NA[b]
Specific surface area (m^2/g)	6.22	12.5

[a] Ube Material Industry Co Ltd.; 1000A.
[b] NA: not analyzed.

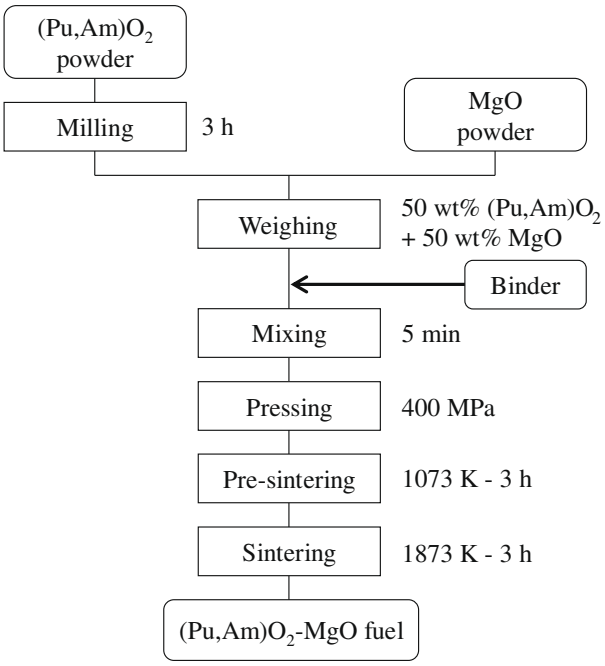

Fig. 1. Fabrication procedure for $(Pu,Am)O_{2-x}$–MgO pellets.

using Al_2O_3 balls, weighing each powder to get the composition of 50 wt% $(Pu,Am)O_2$ and 50 wt% MgO, mixing of these powders for 5 min, cold pressing of the final mixed powder at 400 MPa into a compact and sintering the compact at 1873 K in various sintering atmospheres. The sintering atmospheres were air (AIR), moisturized 4%H_2–Ar (MHA), and 4%H_2–Ar (DHA). Their respective oxygen potentials at 1873 K were about −25 kJ/mol, −387 kJ/mol and −520 kJ/mol.

The $(Pu,Am)O_{2-x}$–MgO pellets sintered in various atmosphere were characterized in term of their densities, diameter profiles, oxygen-to-metal (O/M) ratios of $(Pu,Am)O_{2-x}$ phase, and microstructures.

The sintered densities of the $(Pu,Am)O_2$–MgO pellets were calculated by the following equation:

$$\rho_{TH} = \left(\frac{c_M^W}{\rho_M} + \frac{c_H^W}{\rho_H}\right)^{-1}, \quad (1)$$

where ρ_{TH} is the theoretical density of the composite ($(Pu,Am)O_2$–MgO), and ρ_M and ρ_H are the theoretical densities of the IM (MgO: 3.59 g/cm^3) and host phase ($(Pu_{0.91}Am_{0.09})O_2$: 11.68 g/cm^3), respectively. c_M^W and c_H^W are the weight fractions of the IM (MgO) and host phase ($(Pu,Am)O_2$), respectively. It is assumed in the present study that relative densities of MgO and $(Pu,Am)O_2$ are identical because only two phases, the $(Pu,Am)O_{2-x}$ and the MgO phases, exist based on the following XRD results. The theoretical density of a $(Pu,Am)O_2$–MgO pellet having a composition of 50 wt% MgO and 50 wt% $(Pu,Am)O_2$ is 5.49 g/cm^3.

The sintered density and the diameter profile were obtained from metrological results by using a laser micro gauge and a high accuracy balance. The diameter profile was obtained for 0.5 mm steps in the axial direction of the pellet. The O/M ratio of $(Pu,Am)O_{2-x}$ phase was calculated from the lattice parameter by using Vegard's law, in which $(Pu,Am)O_{2-x}$ was assumed as an ideal solid solution of PuO_2, $PuO_{1.62}$, AmO_2 and $AmO_{1.61}$. Microstructures were observed by ceramography.

3. Results

Fig. 2 plots the density of $(Pu,Am)O_{2-x}$–MgO pellets as a function of oxygen potential in the sintering atmosphere. The results of MgO and PuO_{2-x}–MgO pellets are also given. The density of $(Pu,Am)O_{2-x}$–MgO was significantly affected by oxygen potential while that of PuO_2–MgO and MgO depended little on oxygen potential in the studied range. A high density of the $(Pu,Am)O_2$–MgO pellet of about 94%TD was achieved for AIR. The density of $(Pu,Am)O_{2-x}$–MgO decreased with decreasing oxygen potential in the sintering atmosphere. This meant that the lower density of $(Pu,Am)O_2$–MgO in a reductive atmosphere could be attributed to the effect of Am addition.

Fig. 3 shows the diameter profiles of $(Pu,Am)O_{2-x}$–MgO pellets for AIR, MHA and DHA. The $(Pu,Am)O_{2-x}$–MgO pellet for AIR was well densified, while the $(Pu,Am)O_{2-x}$–MgO pellet for MHA was

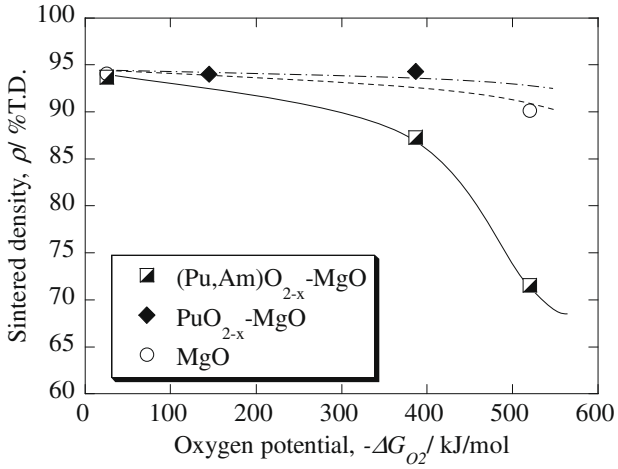

Fig. 2. Sintered density of $(Pu,Am)O_{2-x}$–MgO pellets sintered as a function of oxygen potential in the sintering atmosphere.

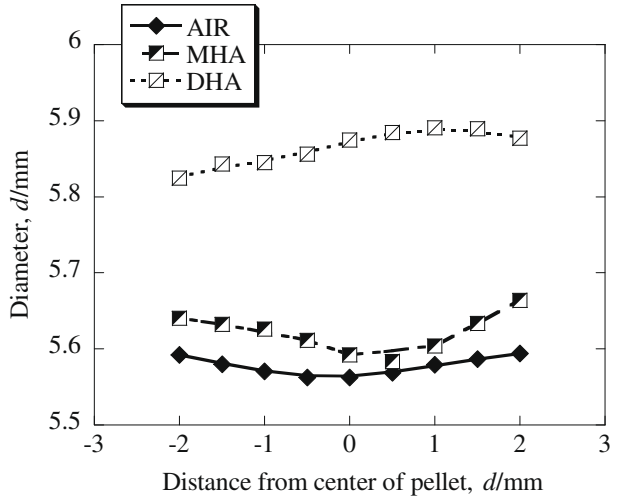

Fig. 3. Diameter profiles of $(Pu,Am)O_{2-x}$–MgO pellets for AIR, MHA and DHA.

only slightly less densified. On the other hand, the profile of the $(Pu,Am)O_{2-x}$–MgO pellet for DHA was completely different from the other two. The pellet for DHA was less densified and swelled in the middle. This is a typical profile for the pellet in which the rate of coarsening increases and larger pores grow. These pores were considered to be trapped in the center of the pellet, and cause pellet swelling in the final sintering stage, as discussed in the next section.

In order to clarify the cause of different density between AIR and MHA which had almost the same profile, microstructure observations were done for $(Pu,Am)O_{2-x}$–MgO pellets for AIR (Fig. 4(a)) and MHA (Fig. 4(b)) as shown in Fig. 4. The light gray-colored image and the dark gray-colored image show the $(Pu,Am)O_{2-x}$ phase and the MgO phase, respectively. The aggregates of $(Pu,Am)O_{2-x}$ host phase for MHA were larger than those for AIR. This meant that the $(Pu,Am)O_{2-x}$ particles coalesced and grain growth progressed much more for MHA than for AIR. On the other hand, larger pores were observed for MHA. The less densification for MHA as shown in Figs. 2 and 3 could be attributed to the formation of these relatively larger pores.

Fig. 5 shows the XRD pattern of $(Pu,Am)O_{2-x}$–MgO pellet for AIR. There were only peaks derived from the halite structure for MgO and fluorite structure for $(Pu,Am)O_{2-x}$. No reaction phase with MgO and $(Pu,Am)O_{2-x}$ was observed. Table 2 lists the lattice parameters and O/M ratios of $(Pu,Am)O_{2-x}$. $(Pu,Am)O_{2-x}$ phase for AIR was near stoichiometry. The O/M ratio of $(Pu,Am)O_{2-x}$ phase for MHA were about 1.93. The $(Pu,Am)O_{2-x}$ for DHA consisted of two phases of two different fluorite structures. This two-phase structure has also been observed when $(Pu,Am)O_{2-x}$ solid solution was heat treated in a reductive atmosphere [16]. These results showed that the $(Pu,Am)O_{2-x}$ were reduced in a low oxygen potential, especially in DHA.

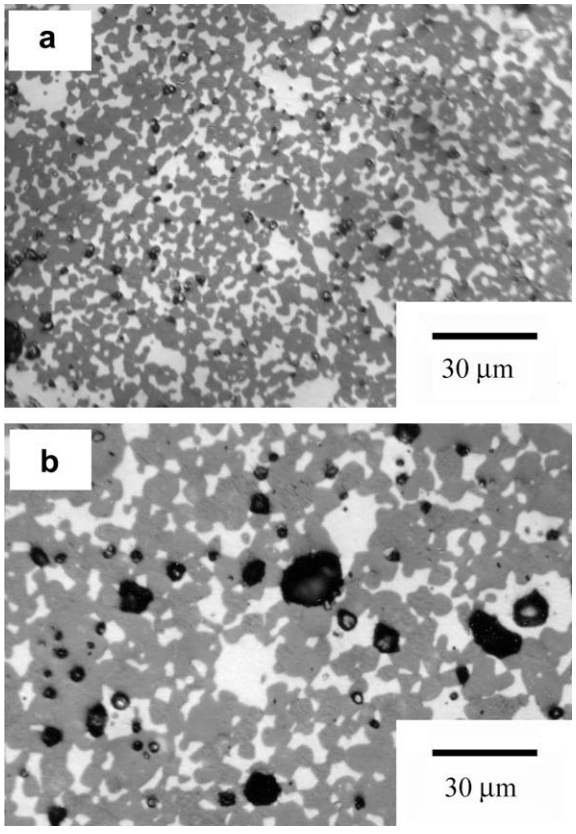

Fig. 4. Ceramographic images of $(Pu,Am)O_{2-x}$–MgO pellets for (a) AIR and (b) MHA.

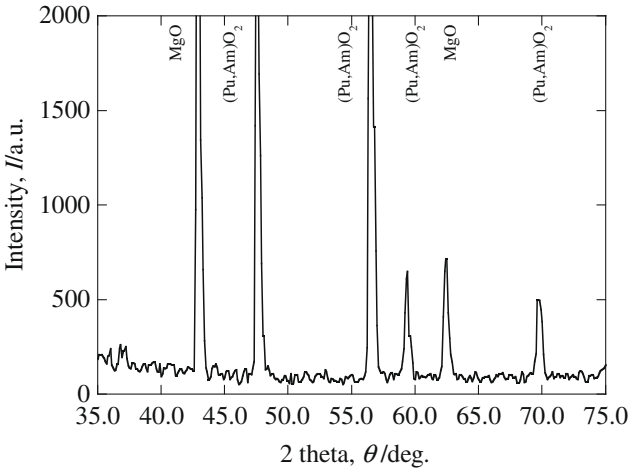

Fig. 5. XRD pattern of $(Pu,Am)O_{2-x}$–MgO pellet for AIR.

Table 2
Lattice parameter and O/M ratio of $(Pu,Am)O_{2-x}$.

Sintering atmosphere	Oxygen potential at 1873 K (kJ/mol)	Lattice parameter (nm)	O/M ratio[a]
Air (AIR)	−25	0.5398	1.99
Moisturized 4%H_2–Ar (MHA)	−387	0.5418	1.93
4%H_2–Ar (DHA)	−520	(0.5418)[b]	(1.93)[b]
		(0.5405)[b]	(1.97)[b]

[a] Calculated by Vegard's law.
[b] The peaks overlapped.

4. Sintering behavior of $(Pu,Am)O_{2-x}$–MgO

It was observed that the sintering behavior of $(Pu,Am)O_{2-x}$–MgO was significantly affected by oxygen potential in the sintering atmosphere. This could be attributed to the growth of pores in the matrix by a mismatch of the densification between $(Pu,Am)O_{2-x}$ and MgO, which would be caused by the dependence of sintering behavior of the $(Pu,Am)O_{2-x}$ on oxygen potential. In this section, the sintering mechanism of $(Pu,Am)O_{2-x}$–MgO is discussed in terms of the difference of the sintering behavior between $(Pu,Am)O_{2-x}$ and MgO under various oxygen potentials.

The sintering process consists of multiple transport processes, i.e. a surface diffusion process, a vaporization–condensation process, a grain boundary diffusion process and so on. Among them, grain boundary diffusion and lattice diffusion from the grain boundary to the pore are the most important mechanisms for the densification. They are controlled by the much slower movement of metal cations than that of oxygen anions in oxides [18].

The sintering behavior of oxides with fluorite structure such as UO_2, PuO_2 and MOX, is known to be affected by oxygen potential [10–12], and this feature in non-stoichiometric oxide fuels with the fluorite structure has been explained by a defect model [19,20]. Namely, the existence of defects such as vacancies, interstitials and clusters enhanced the cation diffusion. Previous work showed that the PuO_2 densification rate was enhanced well in a reductive atmosphere, and it was associated with the presence of defect structures as PuO_2 was reduced to PuO_{2-x} [11]. On the other hand, the Am addition to PuO_{2-x} was found to increase the oxygen potential, especially near stoichiometry [15]. This indicated that $(Pu,Am)O_{2-x}$ could be more easily reduced than PuO_{2-x}. Therefore, $(Pu,Am)O_{2-x}$ host phase could be more sensitive to oxygen potential than PuO_{2-x} host phase. From these considerations, it is believed that the number of defects in $(Pu,Am)O_{2-x}$ host phase

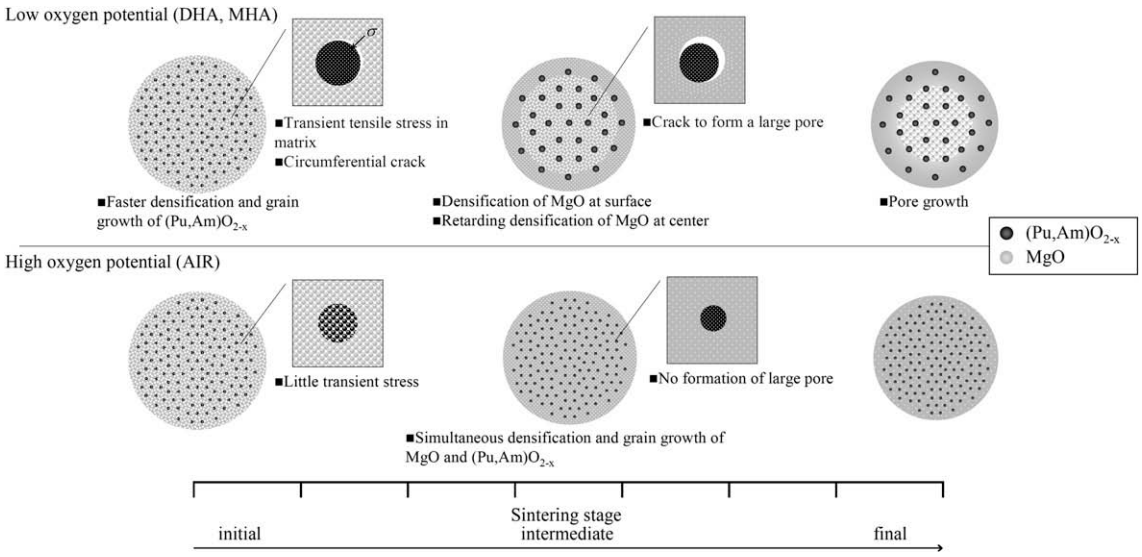

Fig. 6. Schematic drawings showing the sintering mechanism of a $(Pu,Am)O_{2-x}$–MgO pellet sintered under low and high oxygen potentials.

could increase at lower temperature than those of PuO_{2-x}, and could result in the enhancement of sintering in the early sintering stage. This behavior was confirmed by ceramography; the grain growth of $(Pu,Am)O_{2-x}$ host phase was enhanced for $(Pu,Am)O_{2-x}$–MgO pellet sintered in low oxygen potential atmosphere, as shown in Fig. 4(b).

In addition to the above mentioned characteristics, the sintering behavior of heterogeneous fuels is significantly affected by the difference of the sintering behavior between the host phase and the matrix [6–8]. The host phase retards the densification of matrix due to the transient stress in the matrix induced if a mismatch of sintering rate between the host phase and the matrix occurs. This transient stress causes the formation of circumferential cracks in the boundary of the host phase and the matrix [6,7]. Distortion of the cracks leads to formation of a large pore as the sintering proceeds [8].

From this sintering mechanism, the results for PuO_{2-x}–MgO pellets shown in Fig. 2 indicated that densification behavior of PuO_{2-x} powder was like that of MgO powder in this sintering atmosphere range. The sintering of PuO_{2-x} and MgO powders was considered to progress equally, and the transient stress in the matrix may be relaxed, which resulted in the high density of PuO_{2-x}–MgO pellets.

On the other hand, the $(Pu,Am)O_{2-x}$–MgO pellets showed less sintering characteristics in low oxygen potential atmospheres, MHA and DHA. Unlike the PuO_2–MgO, the faster densification and grain growth rate of $(Pu,Am)O_{2-x}$ in low oxygen potential atmosphere should have caused a mismatch of the densification between $(Pu,Am)O_{2-x}$ and MgO.

From these facts, the sintering mechanism of $(Pu,Am)O_{2-x}$–MgO pellet is discussed as below.

Schematic drawings of the sintering mechanism of the $(Pu,Am)O_{2-x}$–MgO pellet are shown in Fig. 6. Under low oxygen potential atmospheres, MHA and DHA, the densification and grain growth of $(Pu,Am)O_{2-x}$ rapidly progressed at lower temperature. In this stage, the transient stress would develop in the MgO matrix around the $(Pu,Am)O_{2-x}$ host phase, and the circumferential cracks would be formed. These phenomena retarded the densification of MgO matrix. On the other hand, the densification at the pellet periphery would be relatively enhanced because the density of pressed compact at the periphery was generally high due to the friction between the compact and the mold. In addition to this behavior, slowing down of the densification of MgO matrix would be suppressed at the pellet periphery by the relaxation of the transient stress because the surface acted as sink for the stress. Therefore, this inhomogeneity of densification behavior of $(Pu,Am)O_{2-x}$–MgO pellet between the center and periphery of the pellet would prevent out-gassing of pores inside the pellet in the intermediate sintering stage, and lead to large pore formation inside the pellet in the final sintering stage. This was confirmed by the relatively large pores seen for MHA as shown in Fig. 4(b). For DHA, the inhomogeneity of densification would be larger. Therefore, larger pores were considered to be trapped in the center of the pellet in the early sintering stage, and they caused pellet swelling as shown in Fig. 3. The lower density of the pellet sintered in low oxygen potential atmosphere was attributable to these pore structures.

Under high oxygen potential atmospheres (AIR), the densification of $(Pu,Am)O_{2-x}$ host phase was considered to be relatively restrained and occurred at almost the same temperature and the same rate as the MgO matrix. The densifications of $(Pu,Am)O_{2-x}$ and MgO were, therefore, equally progressed, which led to relaxation of the transient stress. In the final stage of sintering, the pores would be swept out due to grain growth of respective phases, and high density could be achieved by sintering in high oxygen potential atmospheres.

5. Conclusion

The sintering behavior of the MgO-based heterogeneous fuels containing $(Pu,Am)O_{2-x}$ was experimentally investigated. Sintering tests in air, moisturized 4%H_2–Ar, and 4%H_2–Ar atmosphere were carried out.

The sintering behavior was found to be significantly affected by the sintering atmosphere. The high density was obtained by sintering in high oxygen potential, and the sintered density decreased with decreasing oxygen potential in the sintering atmosphere. This behavior was well interpreted by the sintering mechanism proposed on the basis of the difference in sintering behavior between MgO and $(Pu,Am)O_{2-x}$. It was concluded that a high oxygen potential of the sintering atmosphere was effective for the densification of MgO-based heterogeneous fuels containing $(Pu,Am)O_{2-x}$.

Acknowledgements

The authors wish to thank Mr Kenya Tanaka, Mr Hiroshi Yoshimochi and Mr Kosuke Tanaka of JAEA, Mr Shinichi Sekine of the

Nuclear Technology and Engineering Corporation and Mr Takayuki Seki of the Inspection Development Corporation for their invaluable help in these experiments.

References

[1] M. Osaka, H. Serizawa, M. Kato, K. Nakajima, Y. Tachi, R. Kitamura, S. Miwa, T. Iwai, K. Tanaka, M. Inoue, Y. Arai, J. Nucl. Sci. Technol. 44 (2007) 309.
[2] M. Osaka, S. Miwa, K. Tanaka, I. Sato, T. Hirosawa, H. Obayashi, K. Mondo, Y. Akutsu, Y. Ishi, S. Koyama, H. Yoshimochi, K. Tanaka, in: C.A. Brebbia, V. Popov (Eds.), Energy and Sustainability, Transaction: Ecology and the Environment, vol. 105, Wessex Institute of Technology, UK, 2007, p. 357.
[3] Y. Croixmarie, E. Abonneau, A. Fernandez, R.J.M. Konings, F. Desmouliere, L. Donnet, J. Nucl. Mater. 320 (2003) 11.
[4] M. Osaka, S. Miwa, Y. Tachi, Ceram. Int. 32 (2006) 659.
[5] S. Miwa, M. Osaka, K. Tanaka, Y. Ishi, H. Yoshimochi, K. Tanaka, in: Proceedings of GLOBAL 2007, Boise, USA, September 9–13, 2007, p. 903.
[6] O. Sudre, F.F. Lange, J. Am. Ceram. Soc. 75 (1992) 3241.
[7] R. Raj, R.K. Bordia, Acta Metall. 32 (1984) 1003.
[8] A.G. Evans, J. Am. Ceram. Soc. 65 (1982) 497.
[9] A. Fernandez, R.J.M. Konings, J. Somers, D. Haas, J. Mater. Sci. Lett. 22 (2003) 119.
[10] T.R.G. Kutty, P.V. Hegde, K.B. Khan, U. Basak, S.N. Pillai, A.K. Sengupta, G.C. Jain, S. Majumdar, H.S. Kamath, D.S.C. Purushotham, J. Nucl. Mater. 305 (2002) 159.
[11] T.R.G. Kutty, K.B. Khan, P.V. Hegde, A.K. Sengputa, S. Majumdar, D.S.C. Purushotham, J. Nucl. Mater. 297 (2001) 120.
[12] T.R.G. Kutty, P.V. Hegde, R. Keswani, K.B. Khan, S. Majumdar, D.S.C. Purushotham, J. Nucl. Mater. 264 (1999) 10.
[13] M. Osaka, I. Sato, T. Namekawa, K. Kurosaki, S. Yamanaka, J. Alloys Compd. 397 (2005) 110.
[14] S. Miwa, M. Osaka, H. Yoshimochi, K. Tanaka, T. Seki, S. Sekine, in: I. May, R. Alvares, N. Bryan (Eds.), Recent Advances in Actinide Science, The Royal Society of Chemistry, UK, 2006, p. 400.
[15] M. Osaka, K. Kurosaki, S. Yamanaka, J. Nucl. Mater. 357 (2006) 69.
[16] S. Miwa, M. Osaka, H. Yoshimochi, K. Tanaka, K. Kurosaki, M. Uno, S. Yamanaka, J. Alloys Compd. 444&445 (2007) 610.
[17] T.D. Chikalla, L. Eyring, J. Inorg. Nucl. Chem. 29 (1967) 2281.
[18] M.N. Raraman, Sintering of Ceramics, CRC Press, New York, 2007, p. 46.
[19] Hj. Matzke, in: T. Sorensen (Ed.), Nonstoichiometric Oxides, Academic Press, New York, 1981, p. 156.
[20] Hj. Matzke, J. Chemical Society, Faraday Trans. 86 (1990) 1243.